Comprehensive Control Strategy Design for a Wheelchair Power-Assist Device

Comprehensive Control Strategy Design for a Wheelchair Power-Assist Device

Valerio Cornagliotto(✉), Michele Polito, Laura Gastaldi, and Stefano Pastorelli

Department of Mechanical and Aerospace Engineering, Politecnico di Torino, Turin, Italy
valerio.cornagliotto@polito.it

Abstract. Rear add-ons are assistive devices developed to assist users who have difficulty propelling wheelchairs. Improving the mobility of wheelchair users and allowing them access to more activities is in line with the objective of the sustainable development goals SDG3, and SDG11. Currently, commercial rear add-on devices implement speed-based controls. The speed-based control consists in setting the reference speed that the device must keep constant which makes rear add-on devices suitable for long journeys but, makes them unsuitable for use in narrow spaces. In this paper an hybrid control is presented. The proposed control law takes into account the thrust exerted by the user (torque-based), the forward speed of the wheelchair (speed-based), as well as the surrounding environmental conditions. The total torque delivered by the device is evaluated as the sum of a contribution proportional to the user's thrust, a delayed contribution as a function of forward speed, and the gravity compensation contribution. The proportional contribution synchronous with respect to the user's push at low speeds improves manoeuvrability and controllability of the wheelchair, whereas, at higher speeds, the introduction of the delayed thrust distributes the assistance torque over a longer period, reducing the peak of torque provided by the device. A dynamic multibody model of a wheelchair was also developed and implemented in the Simulink environment to test the proposed control algorithm. As a future step the algorithm will be implemented on a rear add-on device and it will be tested experimentally by wheelchair users.

Keywords: SDG3 · SDG11 · control · multibody · wheelchair · assistive

1 Introduction

Many manual wheelchair users may find it difficult to get around and perform daily activities. Difficulty could be due to reduced physical ability, upper body weakness, pain, injury, or fatigue from prolonged wheelchair pushing. Facilitating wheelchair users' mobility is in line with the aim of the third sustainable development goal (SDG3) healthy lives and promotion of well-being, as well as promoting human settlements inclusive for persons with reduced mobility (SDG11). Previous studies have shown that power assisted devices (PADs) positively affected propulsion capabilities, reducing biomechanical and physiological strain associated with manual wheelchair self-propulsion [1–3] and improving mobility [4]. Currently, there are different types of propulsion assist

V. Petuya et al. (Eds.): I4SDG 2023, MMS 134, pp. 1–9, 2023.
https://doi.org/10.1007/978-3-031-32439-0_19

devices for wheelchairs. The main ones can be divided into three categories: pushrim activated power-assisted wheelchairs (PAPAW), which consist of replacing the standard wheels with two motorized and sensorised wheels; the front-end attachments, which consist of a motorized wheel steered by a handlebar that transforms the wheelchair into a tricycle; rear-end attachments, also called rear add-ons, which consist of a drive wheel placed under the seat in the rear part of the wheelchair. The drive wheel provides an amount of torque sufficient to propel the wheelchair autonomously. In previous studies, the user perception and performance of some of the most common PADs have been investigated [5–11]. The main positive aspects of the add-on devices that have emerged from users' perception are the small size and low weight. However, some gaps in intuitiveness and control reliability have been highlighted. The control laws currently integrated into assistive devices are mainly speed-based control and torque-based control. PAPAW-type devices mainly exploit torque-based controls by acting as torque multipliers. To estimate the action exerted by the user on the wheels, the motorized wheel has built-in sensors. Hence, whenever the user performs a push gesture, the control generates a torque reference for each wheel proportional to the torque exerted on the handrim. By exerting greater action on one of the two wheels, the control generates a different torque reference for the left and the right side, and consequentially the wheelchair steers. To compensate for any kinetic or temporal thrust asymmetries, controls that consider the torque balance ratio have been developed [12]. In addition, some control strategies integrate gravity compensation to assist the user pushing the wheelchair up a ramp [13].

On the contrary, the integrated controls on the rear add-on devices are speed-based. The user sets a speed command and the device sustains the propulsion at the given speed until the user provides input to change the speed or halt the device. In this case, the user can manoeuvre the wheelchair by braking both wheels. In the speed control the gravity is intrinsically compensated because whenever going uphill the device automatically supplies a higher torque to follow the set speed reference.

Overall, torque-based control as a thrust multiplier is more suitable in narrow spaces and for small movements while a more uniform thrust, like the one provided in speed controller, is more suitable for long trips.

In this work, a hybrid-control for assistance devices is presented. The goal is to obtain a comprehensive control law for a power assist device that takes into account the force exerted by the users on the handrim, the ground inclination, and the travel speed. As a result, the assistance device would be able to provide more suitable assistance according to the user's needs and to adapt continuously to external conditions.

2 Dynamic Model

A standard reference wheelchair (14 kg and 24 inches wheels diameter), a multibody dummy 50^{th} percentile Italian male, and a rear add-on device were conceived as multibody dynamic models and implemented in Simulink Simscape (Fig. 1), as described in the previous work [14].

The wheelchair dynamic behavior is mainly influenced by the forces exerted by the user on the handrims, the additional thrust provided by the rear add-on device, and losses. In particular, losses can be due to rolling friction, air drag, and viscous losses in the wheels

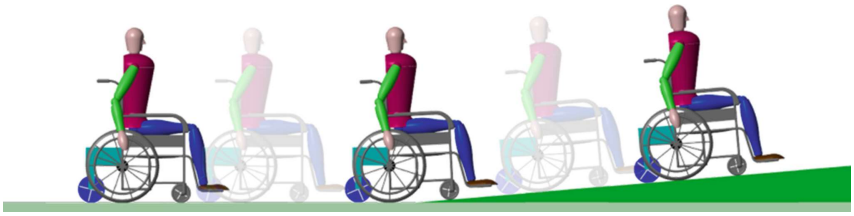

Fig. 1. Virtual representation of the multibody dynamic model

bearings. The contact between tyres and ground was modelled as a stick-slip continuous contact model (μ_s: static friction coefficient, μ_d: dynamic friction coefficient) and a visco-elastic model was adopted for tyre deformation (k_{tyre}: stiffness, c_{tyre}: damping). The rolling friction force F_{roll} was modelled as Eq. (1):

$$F_{roll} = c_{roll} F_N \tag{1}$$

where c_{roll} is the rolling coefficient and F_N is the normal contact force between the wheel and the ground. The estimation of the rolling friction values can be non-trivial due to many non-linearities; many previous works have investigated the link between rolling friction and tyre type, ground, speed, and other dependencies [15, 16]. The viscous damping torque $T_{\omega i}$ has been applied on the two wheels and defined as Eq. (2):

$$T_{\omega i} = \eta_v \omega_i \tag{2}$$

where η_v is a loss coefficient set according to [17] and ω_i is the wheel angular speed. The air resistance F_{air} was defined as in Eq. (3).

$$F_{air} = \frac{1}{2} v^2 C_D A \rho \tag{3}$$

where C_D is a form factor and A is the frontal area [16], v is the wheelchair speed, and ρ the air density.

The force exerted by the user has been modelled as a sinusoidal function saturated positive, with the push pattern consistent with the results presented in [18]. The main features considered (Table 1) are the cycle time C_{time}, the push phase P_p, the peak tangential force $F_{t\,peak}$, and the mean tangential force $F_{t\,mean}$ The resulting handrim tangential force $\boldsymbol{F_t}$ is shown in Eq. (4).

$$\boldsymbol{F_t} = \max\left(0; F_{tpeak} \sin\left(\frac{2\pi}{C_{time}} t - \frac{\pi}{2}\right) - bias\right) \tag{4}$$

Table 1. Push gesture parameters

Parameters	$\boldsymbol{C_{time}}$ (s)	P_p (%)	$F_{t\,peak}$ (N)	$F_{t\,mean}$ (N)
	1.15	36	33	21

The additional thrust provided by the add-on is defined as a function of F_t, speed, and wheelchair inclination. The assistive torque produced by the rear add-on device is transmitted to the wheelchair through a revolute joint coaxial to the wheels. The control law will be described deeper in the specific section. In order to find the optimal parameters that fit the wheelchair behaviour in lab trials, deceleration test have been performed. The experimental test showed a decay of the linear speed of the free wheelchair from 0.9 m/s to 0 m/s in approximately 9 s as shown in Fig. 2a. Hence, a curve fitting procedure was carried out, and all the optimal parameters were set as shown in Table 2. To validate the model an experimental test consisting in 8 pushes from standstill was performed and the forces exerted by the user on the handrims and the wheel speed were acquired by suitable sensors embedded in the wheels. The forces during trial were provided as input to the model. The wheelchair speed acquired experimentally and the one estimated through the simulation were compared. Numerical results well approximate the experimental data (Fig. 2b).

Table 2. Model optimal parameters

k_{tyre} (N/m)	c_{tyre} (Ns/m)	η_v(Nms/rad)	μ_s	μ_d	Front c_{roll}	Rear c_{roll}
3e5	1e4	0.05	0.85	0.65	0.012	0.007

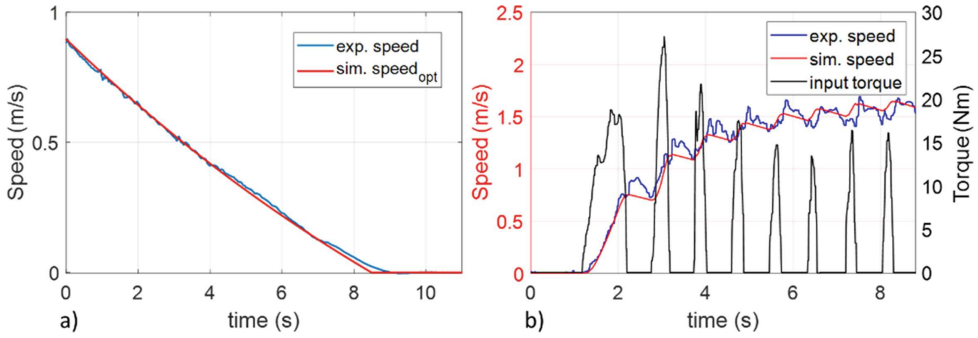

Fig. 2. Experimental and simulated angular velocity decay (a), model validation output (b)

3 Control Law

The control law of the add-on device is designed as described in Eq. (5)

$$\boldsymbol{T_{addon}}(t, v, \alpha) = \left(\boldsymbol{T_H}(t)\left(a_1 - \frac{a_1\delta}{2\delta_{max}}\right) + \boldsymbol{T_H}(t-\delta)\left(\frac{a_1\delta}{2\delta_{max}}\right)\right) \cdot(1 - b_1\alpha) + M_{tot}g\sin(\alpha)r \tag{5}$$

$$\delta = \max(0; \min(d_1 v - d_2; \delta_{max})) \tag{6}$$

where $\boldsymbol{T_H}(t) = \boldsymbol{F_t}(t)R$ is the human torque provided at the handrims, δ is a delay factor described in Eq. (6), r is the radius of the add-on wheel, R is the radius of the wheelchair

Table 3. Control law parameters

Parameters	$a1$	b_1(rad^{-1})	d_1(s^{2}m^{-1})	d_2(s)	δ_{max} (s)	r (m)	R (m)	M_{tot}(kg)
	0.75	6.02	0.67	0.17	0.25	0.11	0.26	89,2

wheels, M_{tot} is the total mass, v is the linear speed of the wheelchair, and a_1, b_1, d_1, d_2, and δ_{max} are coefficients. The values of all parameters are defined in Table 3.

The total torque $\boldsymbol{T_{addon}}$ consists of three main contributions: proportional (P), delayed (Δ), and gravity compensation (G). P makes the add-on device responsive to fast changes in input torque and is the only contribution at low speed ($v < 0.25$ m/s). Δ makes the speed ripple smoother as the assistance torque lasts longer than the human torque. The introduction of Δ contribution makes the assistance more suitable for higher speed in steady state conditions. G is introduced to compensate gravity when the wheelchair is on a ramp. It prevents the rolling back of the wheelchair and reduces the effort of the user going on graded roads. In order to have a more continuous torque, the value of the gains of P and Δ are proportional to the delay. In particular, the P gain is decreasing with the delay whereas the Δ gain is increasing. An overall gain of the sum of P and Δ contributions is applied in order to decrease the maximum torque on the graded surface. The overall gain is equal to 0.5 when the wheelchair inclination reaches 4.8° (which is the maximum inclination angle of ramps according to ISO 21542:2021). That adjustment decreases the speed upward giving the user the perception of going uphill.

4 Results and Discussions

The first simulation was done with no assistance by introducing the forces exerted by the user to propel the wheelchair on a levelled surface as described in Sect. 2. A steady state speed of 2.1 m/s is obtained as shown in Fig. 3a.

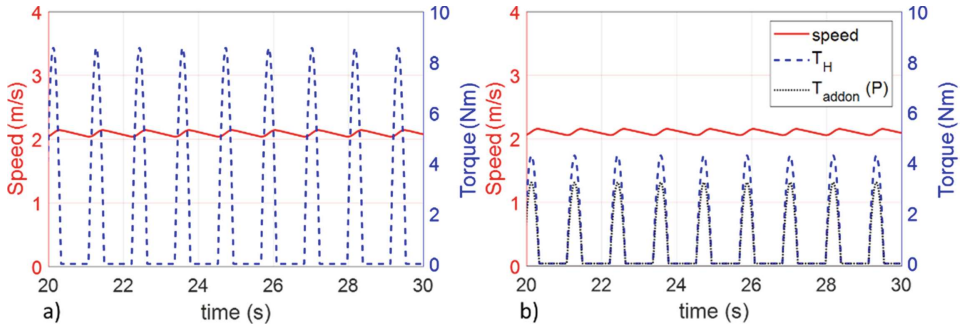

Fig. 3. Steady-state speed and provided torques without assistance (a) and with assistance (b)

Then, the assistance thrust of the device has been introduced. To evaluate the value of the a_1 coefficient, a simulation with only the P contribution was performed. The value of a_1 was estimated to obtain the same steady-state speed when 50% of the torque is exerted by the user as shown in Fig. 3b. Then, the Δ contribution was introduced (Fig. 4).

The δ_{max} was set equal to 0.25 s, which corresponds to about a quarter of the period of the push phase. d_1 and d_2 were chosen in order to have the delay starting above 0.25 m/s and the maximum delay at 0.60 m/s. To limit the sum of P and Δ when the two contributions overlap, the gain proportional to $\boldsymbol{T_H}$. Was adjusted proportionally to the delay. In the maximum-delay condition, the P gain is halved with respect to the no-delay condition. The Δ gain is proportional to the delay and its maximum value was set to be equal to P evaluated in the maximum-delay condition.

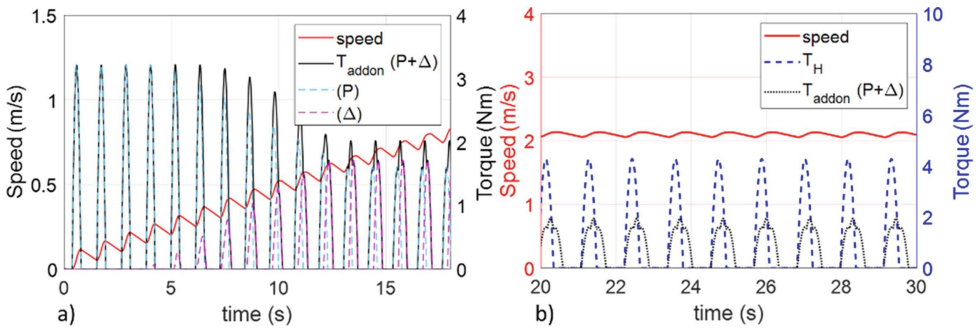

Fig. 4. Transient (a); steady-state (b)

Analysing the speed trend and the torque delivered by the device it can be inferred how it is possible to obtain a smoother ripple at the same average speed (Fig. 5a) by delivering about half of the peak torque (Fig. 5b). Moreover, even if the maximum transmissible torque increases as the assistive torque increases [14], reducing the peak torque can be an advantage in low grip conditions to avoid wheel slippage.

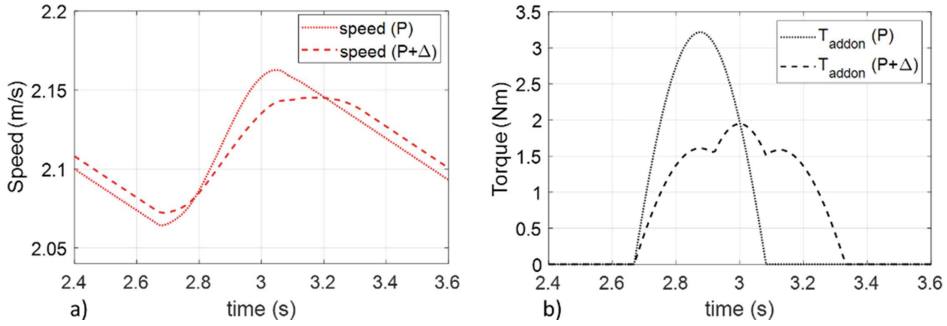

Fig. 5. Speed ripple comparison (left); torque comparison (right)

Eventually, the G gravity compensation was introduced. The amount of assistive torque to compensate for the force of gravity has been estimated analytically by imposing the wheelchair to be still on a ramp without any additional torque exerted by the user. Hence, a simulation of the wheelchair approaching an 8% graded surface was carried out. The total assistive torque is equal to the sum of the three contributions, in particular, the G contribution is highlighted in Fig. 6.

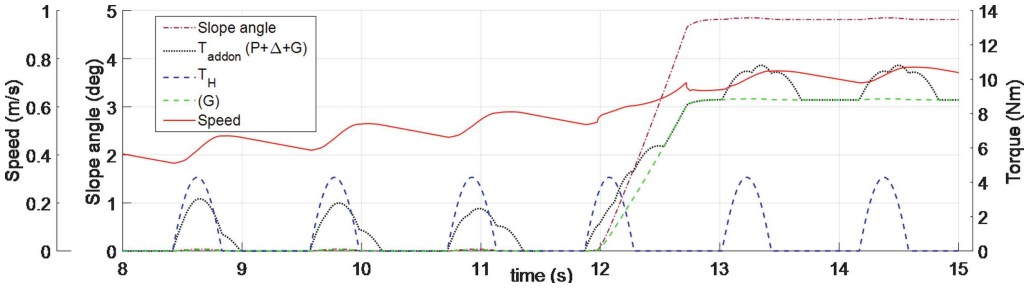

Fig. 6. Complete additional torque control law

5 Conclusions

The development of a comprehensive control algorithm that adapts to user actions as well as environmental conditions is essential to make rear add-on devices more intuitive and all-round. In this paper, a control law that takes into account the action that the user exerts on the handrims, the forward speed, and the pitch angle of the wheelchair is presented. The total torque delivered by the device is calculated as the sum of three contributions: proportional to the user's thrust, delayed as a function of forward speed, and gravity compensation. At low speeds the torque is purely proportional and synchronous with the user's thrust, improving the controllability and manoeuvrability in narrow spaces. At higher speeds, the assistance torque is distributed over a longer period than the user's thrust period, guaranteeing a more gradual and more suitable assistance for longer distances. A dynamic multibody model of a wheelchair was developed and implemented in the Simulink environment to design the control algorithm. At the moment the algorithm is being implemented on a rear add-on prototype (patent pending) designed by authors and experimental tests are being carried out with actual users. Hence, it will be possible to tune optimised control parameters on the basis of the subjects' perceptions.

Acknowledgments. This research was partially conducted within the project "Advanced Light Body Assistants - Sistema avanzato leggero per l'assistenza a persone diversamente abili"- P.O.R. FESR 2014/2020 - Azione I.lb.2.2 Bando Pi.Te.F.

References

1. Algood, S.D., Cooper, R.A., Fitzgerald, S.G., Cooper, R., Boninger, M.L.: Effect of a pushrim-activated power-assist wheelchair on the functional capabilities of persons with tetraplegia. Arch. Phys. Med. Rehabil. **86**(3), 380–386 (2005). https://doi.org/10.1016/j.apmr.2004.05.017
2. Cooper, R.A., et al.: Evaluation of a pushrim-activated, power-assisted wheelchair. Arch. Phys. Med. Rehabil. **82**(5), 702–708 (2001). https://doi.org/10.1053/apmr.2001.20836
3. Algood, S.D., Cooper, R.A., Fitzgerald, S.G., Cooper, R., Boninger, M.L.: Impact of a pushrim-activated power-assisted wheelchair on the metabolic demands, stroke frequency, and range of motion among subjects with tetraplegia. Arch. Phys. Med. Rehabil. **85**(11), 1865–1871 (2004). https://doi.org/10.1016/j.apmr.2004.04.043

4. Levy, C.E., Buman, M.P., Chow, J.W., Tillman, M.D., Fournier, K.A., Giacobbi, P., Jr.: Use of power assist-wheels results in increased distance traveled compared to conventional manual wheeling. Phys. Med. Rehabil. Serv. **89**(8), 625–634 (2010). https://doi.org/10.1097/PHM.0b013e3181e72286
5. Khalili, M., Eugenio, A., Wood, A., Van der Loos, M., Mortenson, W.B., Borisoff, J.: Perceptions of power-assist devices: interviews with manual wheelchair users. Disabil. Rehabil. Assist. Technol. 1–11 (2021). https://doi.org/10.1080/17483107.2021.1906963
6. Flockhart, E.W., Miller, W.C., Campbell, J.A., Mattie, J.L., Borisoff, J.F.: Evaluation of two power assist systems for manual wheelchairs for usability, performance and mobility: a pilot study. Disabil. Rehabil. Assist. Technol. 1–13 (2021). https://doi.org/10.1080/17483107.2021.2001063
7. Khalili, M., Kryt, G., Mortenson, W.B., Van der Loos, H.F.M., Borisoff, J.: Comparison of manual wheelchair and pushrim-activated power-assisted wheelchair propulsion characteristics during common over-ground maneuvers. Sensors **21**(21), 7008 (2021). https://doi.org/10.3390/S21217008
8. Sawatzky, B., Mortenson, W.B., Wong, S.: Learning to use a rear-mounted power assist for manual wheelchairs. Disabil. Rehabil. Assist. Technol. **13**(8), 772–776 (2017). https://doi.org/10.1080/17483107.2017.1375562
9. Kloosterman, M.G., Buurke, J.H., Schaake, L., Van der Woude, L.H., Rietman, J.S.: Exploration of shoulder load during hand-rim wheelchair start-up with and without power-assisted propulsion in experienced wheelchair users. Clin. Biomech. **34**, 1–6 (2016). https://doi.org/10.1016/j.clinbiomech.2016.02.016
10. Cooper, R.A., et al.: Performance assessment of a pushrim-activated power-assisted wheelchair control system. IEEE Trans. Control Syst. Technol. **10**(1), 121–126 (2002). https://doi.org/10.1109/87.974345
11. Best, K.L., Kirby, R.L., Smith, C., Macleod, D.A.: Comparison between performance with a pushrim-activated power-assisted wheelchair and a manual wheelchair on the Wheelchair Skills Test. Disabil. Rehabil. **28**(4), 213–220 (2009). https://doi.org/10.1080/09638280500158448
12. Heo, Y., Hong, E.P., Chang, Y.H., Jeong, B., Mun, M.S.: Experimental comparison of torque balance controllers for power-assisted wheelchair driving. Measurement **120**, 175–181 (2018). https://doi.org/10.1016/j.measurement.2018.02.024
13. Lee, K.M., Lee, C.H., Hwang, S., Choi, J., Bang, Y.B.: Power-assisted wheelchair with gravity and friction compensation. IEEE Trans. Ind. Electron. **63**(4), 2203–2211 (2016). https://doi.org/10.1109/TIE.2016.2514357
14. Cornagliotto, V., Perino, F., Gastaldi, L., Pastorelli, S.: Evaluation on implementing an active braking system in wheelchair rear-mounted power-assisted device. In: Müller, A., Brandstötter, M. (eds.) Advances in Service and Industrial Robotics (RAAD 2022). Mechanisms and Machine Science, vol. 120, pp. 351–358. Springer, Cham (2022). https://doi.org/10.1007/978-3-031-04870-8_41
15. Sauret, C., et al.: Assessment of field rolling resistance of manual wheelchairs (2014). To cite this version : HAL Id : hal-01086723 Science Arts & Métiers (SAM)
16. Hoffman, M.D., Millet, G.Y., Hoch, A.Z., Candau, R.B.: Assessment of wheelchair drag resistance using a coasting deceleration technique. Am. J. Phys. Med. Rehabil. **82**(11), 880–889 (2003). https://doi.org/10.1097/01.PHM.0000091980.91666.58

17. Nguyen, V.T., Bentaleb, T., Sentouh, C., Pudlo, P., Popieul, J.C.: On a complete dynamical model of manual wheelchair for virtual reality simulation platform. In: 2019 IEEE International Conference on Systems, Man and Cybernetics (SMC), pp. 2417–2422. IEEE (2019). https://doi.org/10.1109/SMC.2019.8913960
18. Soltau, S.L., Slowik, J.S., Requejo, P.S., Mulroy, S.J., Neptune, R.R.: An investigation of bilateral symmetry during manual wheelchair propulsion. Front. Bioeng. Biotechnol. **3**, 86 (2015). https://doi.org/10.3389/fbioe.2015.00086